CFD simulation report

1. Project information

Field	Value
Project title	Benchmark circular cylinder
Project description	Reference: Henderson (1995)
Simulation ID	80d0ef8e-f887-40ad-ab95-abb94a180926
Report generated	2026-07-07 15:29 CEST

Contents

2. Scope

Dimensionless aerodynamic fingerprint of the building geometry from a virtual digital wind tunnel.

This solver operates as a virtual digital wind tunnel, extracting the fundamental aerodynamic fingerprint of your building geometry. The report delivers pure, dimensionless aerodynamic coefficients (C_p, and where applicable C_D, C_L, and Strouhal numbers n_s) that integrate into any global design standard, whether ASCE 7, Eurocode 1, or local structural frameworks. We supply the exact geometric behaviour; you apply your local environmental safety factors.

3. Methodology

The simulation reproduces uniform approach flow past your geometry in a two-dimensional virtual wind tunnel. Reported C_p, C_D, C_L, and n_s are dimensionless coefficients extracted from the computed flow field. They describe the aerodynamic fingerprint of this section and are intended for use with your chosen design code and local safety factors. They are not tied to a prescribed wind speed or air density in this report.

Applicability. The model treats the geometry as an infinite prismatic strip (2D section normal to the span direction). This is appropriate when the along-span aspect ratio is large (typically AR > 5). For shorter bodies, three-dimensional tip and corner effects are not captured.

Conservatism vs. 3D. Sectional coefficients from a 2D strip study tend to be conservative for windward drag and peak suction on long facades, because tip relief and flow three-dimensionality are omitted. Where end effects or corner vortices govern the design, a dedicated 3D study is required.

3.1. Simulation setup

Parameter	Value
Grid resolution	1792 × 1472
Timesteps	200000
Blockage ratio	3.4%

3.2. Domain

Geometry extent and lattice discretization in project length units. Spatial coordinates in field plots use the same unit system.

Parameter	Value
Domain extent (X × Y)	36.5 × 30 m
Lattice spacing Δx	0.02038 m

3.3. Obstacle indexing

Connected obstacle components from the raster mask, ordered streamwise ($+x$). Indices match the coefficient tables below and boundary C_p figures in the flow-field section.

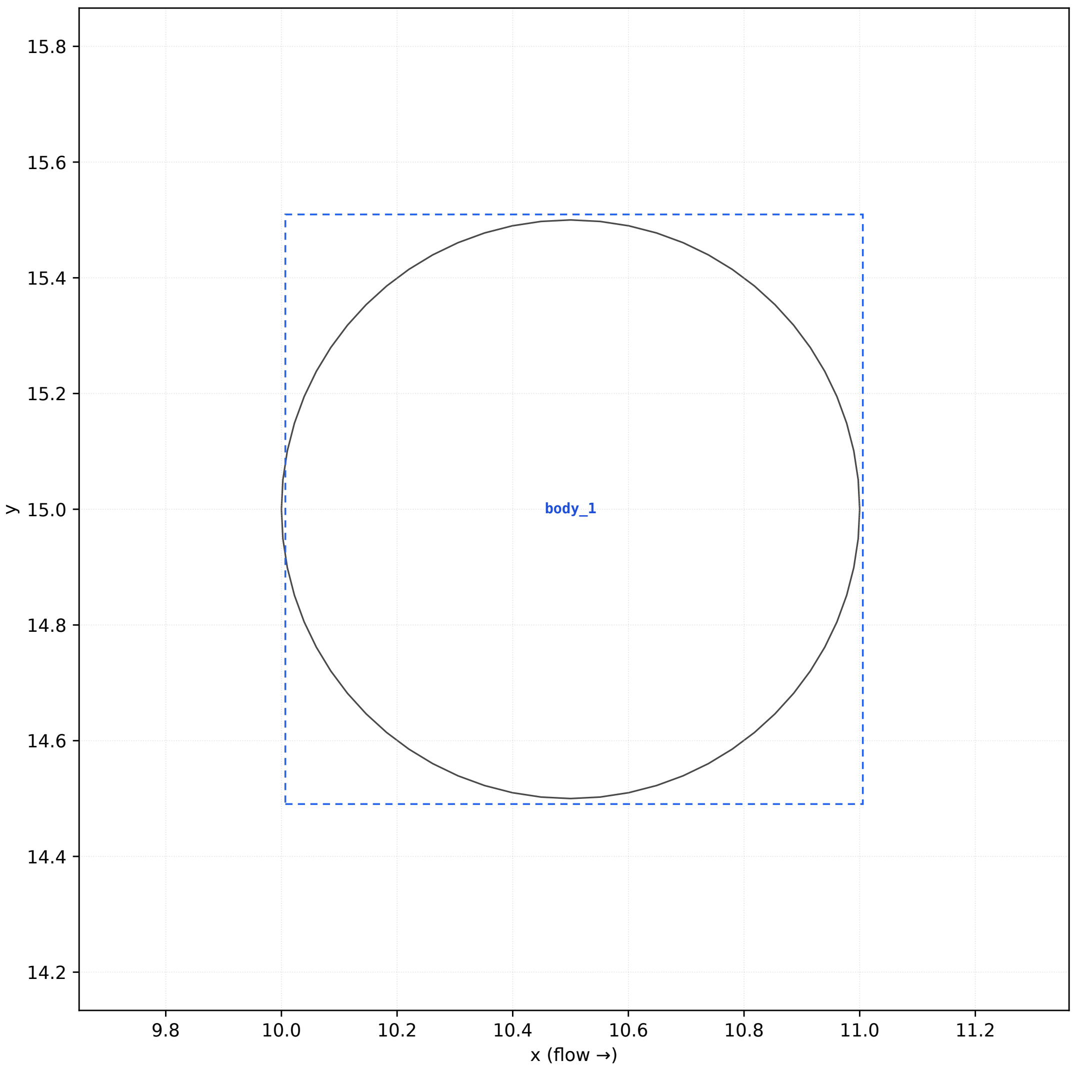

Figure 1: Source geometry with bounding boxes and body indices.

Coefficient selection (EN 1991-1-4). Open-flow / elevated geometry: use momentum-exchange C_D and C_L for overall section forces and vortex-shedding checks (EN1991-1-4:2005). Pressure-based coefficients are included for surface pressure mapping. Steps 1–25600 were omitted before the shedding FFT and the mean force coefficients. Mean C_D and C_L use steps 25601–199984. Pressure C_p is from the final timestep only.

3.4. Zone-mean pressure coefficients

External pressure coefficients on windward and leeward facets (EN 1991-1-4 external pressures).

Location	Obstacle ind.	C_p,front	C_p,rear	C_p,net
Obstacle	body_1	+0.21	-0.85	**+1.06**

3.5. Momentum-exchange force coefficients ($C_{D,\mathrm{MEA}}$, $C_{L,\mathrm{MEA}}$)

Time-averaged momentum exchange on obstacle links; same D and A_{ref} as pressure integration. **Recommended for this open-flow / elevated geometry (EN1991-1-4:2005).**

Object	Obstacle ind.	$C_{D,\mathrm{MEA}}$	$C_{L,\mathrm{MEA}}$
Obstacle	body_1	**+1.382**	+0.002

3.5.1. Streamwise shielding factors

Shielding factors compare time-mean MEA drag coefficients for geometrically identical obstacles at different streamwise positions: $S_i = \frac{C_{D,\mathrm{MEA},i}}{C_{D,\mathrm{MEA,baseline}}}$, where the baseline is the upstream-most duplicate (smallest x). Values below 1.0 indicate reduced drag from wake shielding (e.g. stacked solar panels or cylinder rows). No repeating obstacle shapes were detected at different streamwise positions; shielding factors require at least two geometrically identical bodies.

Object	Obstacle ind.	Baseline	Shielding factor S
Obstacle	body_1	—	N/A

4. Flow fields

4.1. Figures

4.1.1. Pressure coefficient (Cp)

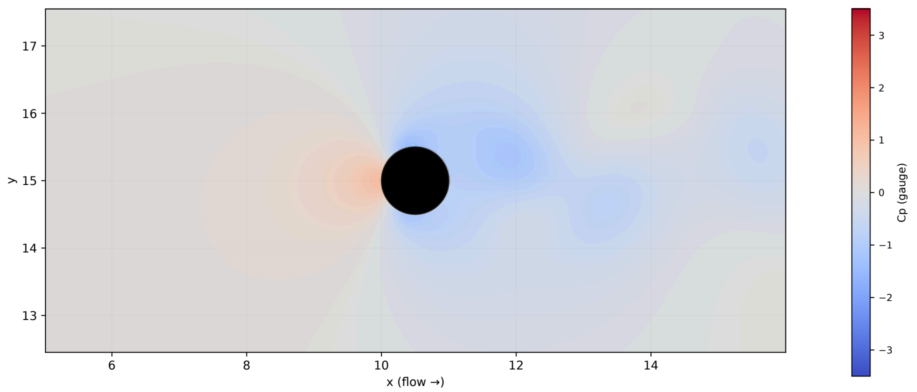

Figure 2: Gauge pressure coefficient near obstacles (5× streamwise, 2× vertical padding).

4.1.2. Velocity magnitude

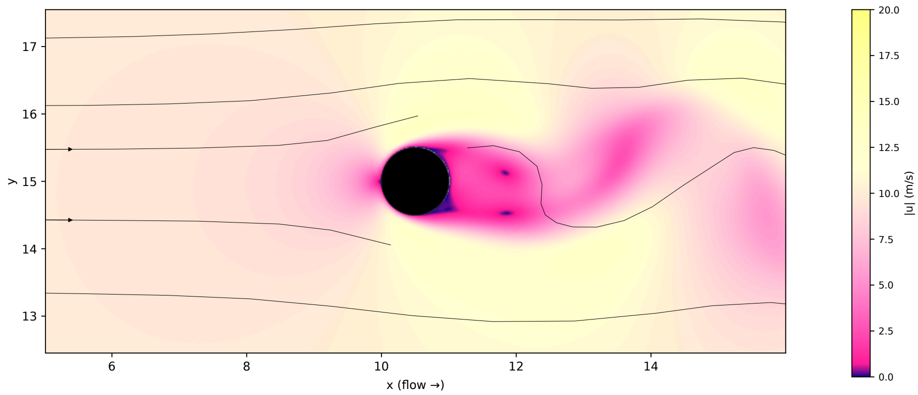

Figure 3: Speed field with streamlines near obstacles (5× streamwise, 2× vertical padding).

4.1.3. Vorticity

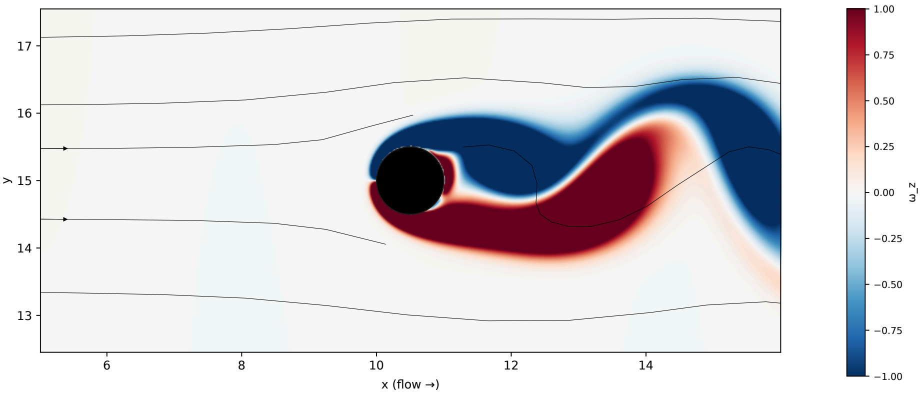

Figure 4: Normalized vorticity near obstacles (5× streamwise, 2× vertical padding).

4.1.4. Boundary Cp, body_1

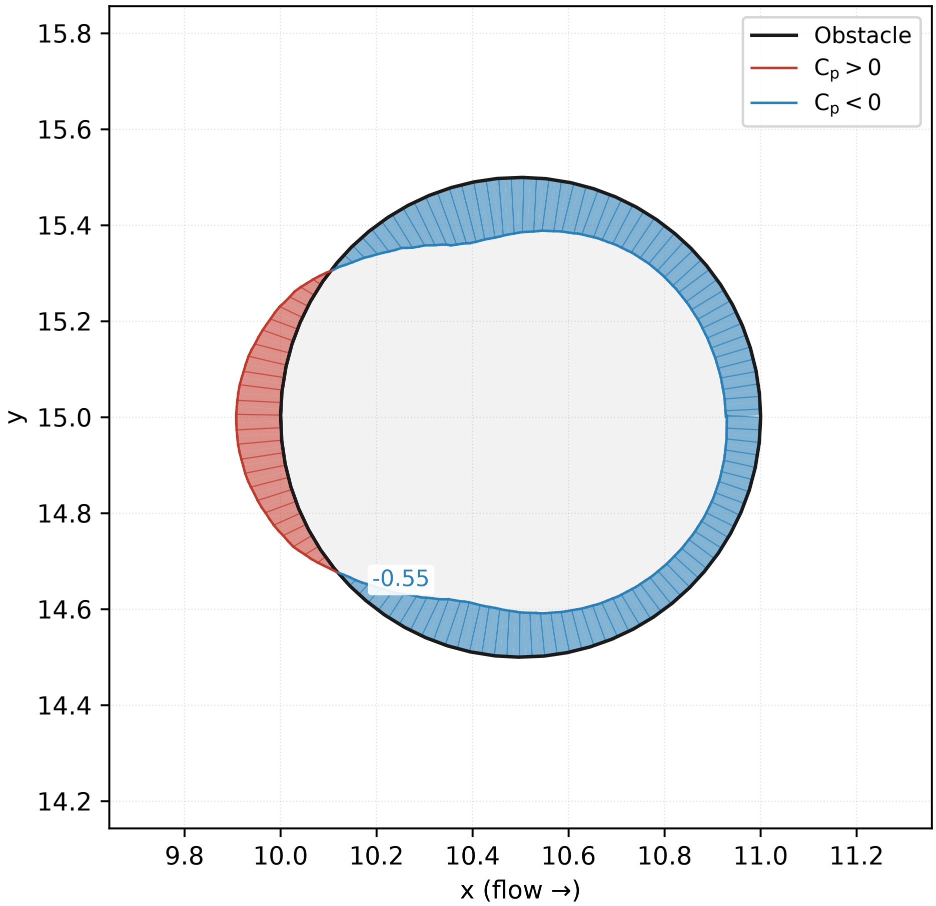

Figure 5: Cp ribbon along obstacle perimeter. Map localized pressures to cladding and facade design.

4.2. Vortex shedding

Cross-wind vortex shedding per EN1991-1-4:2005. Peak shedding frequency f and Strouhal number $n_s = f\frac{b}{U}$ from the across-wind force fluctuation spectrum. Characteristic dimension b is the structure extent perpendicular to the wind direction ($+x$).

body_1 — Developed shedding (converged)

Quantity	Value
Peak shedding frequency f	**1.69 Hz**
Strouhal number n_s	**0.172**
Characteristic dimension b	**1.02 m**

4.2.1. Across-wind force spectrum

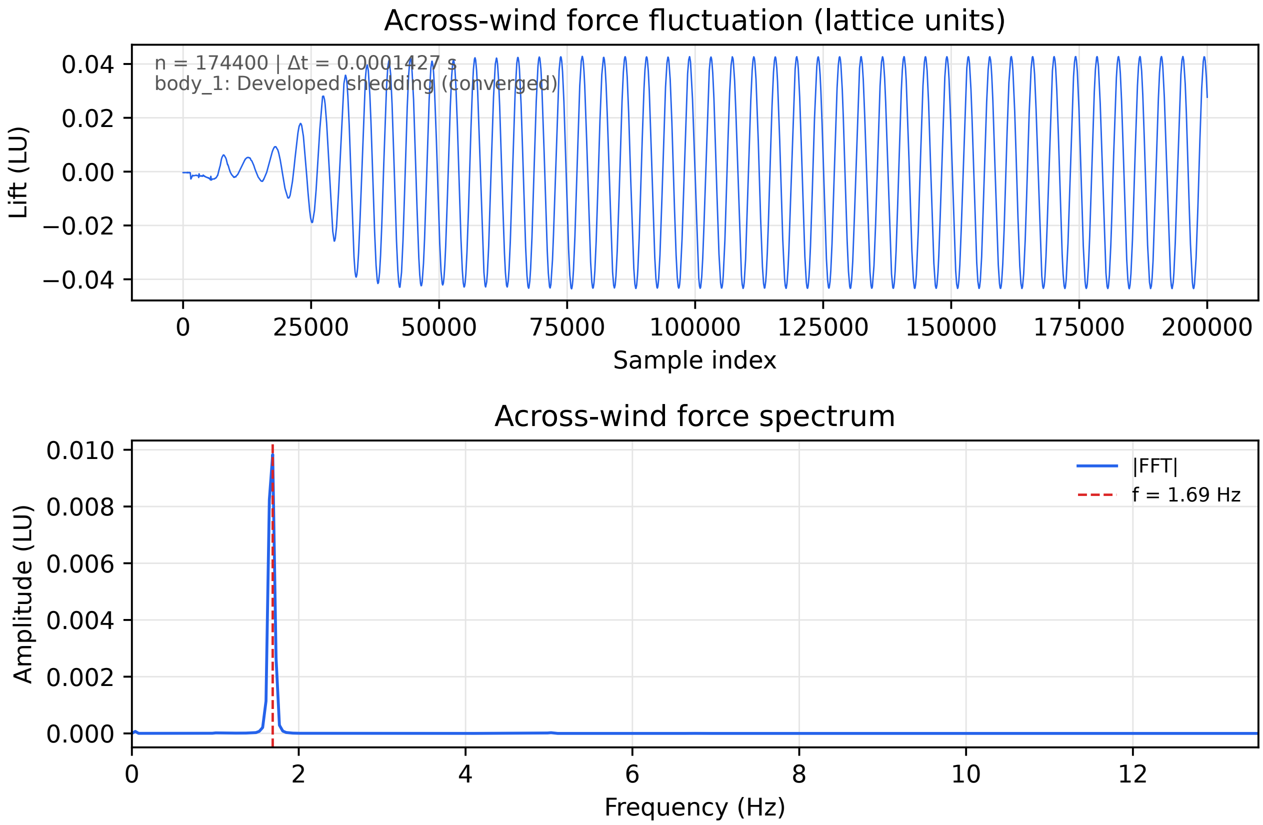

Figure 6: Cross-wind force fluctuation time history and frequency spectrum (EN1991-1-4:2005).

5. Annex: full-domain flow fields

Full computational-domain views of the field plots shown zoomed in the flow-field section. Use these figures to inspect the complete wind-tunnel extent and far-field behaviour.

5.0.1. Pressure coefficient (Cp) (full domain)

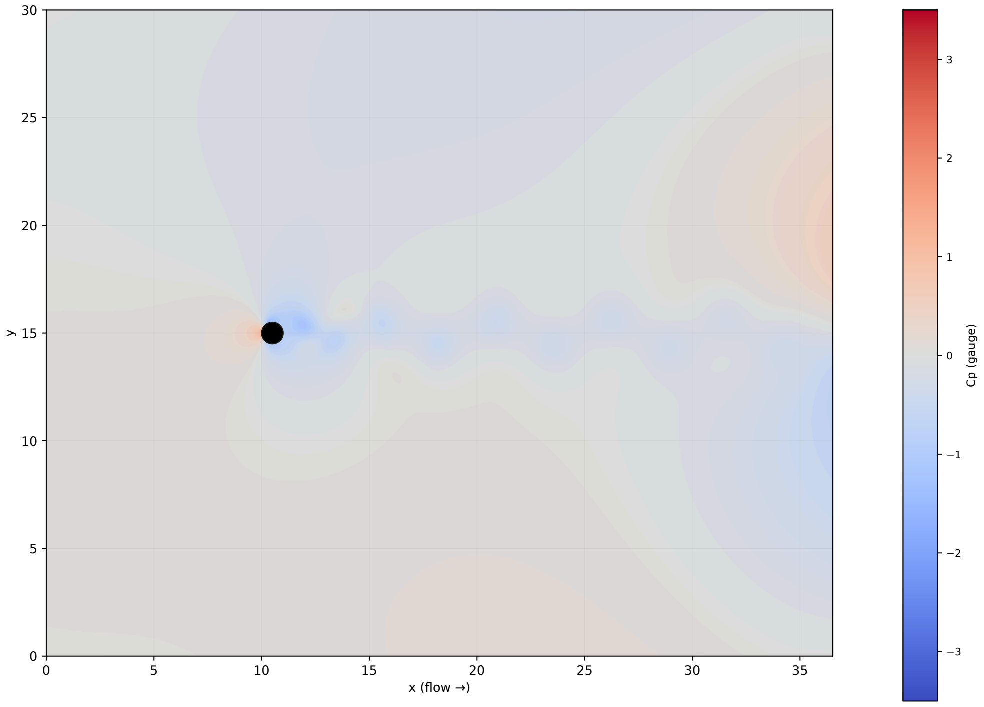

Figure 7: Full-domain gauge pressure coefficient at the final timestep.

5.0.2. Velocity magnitude (full domain)

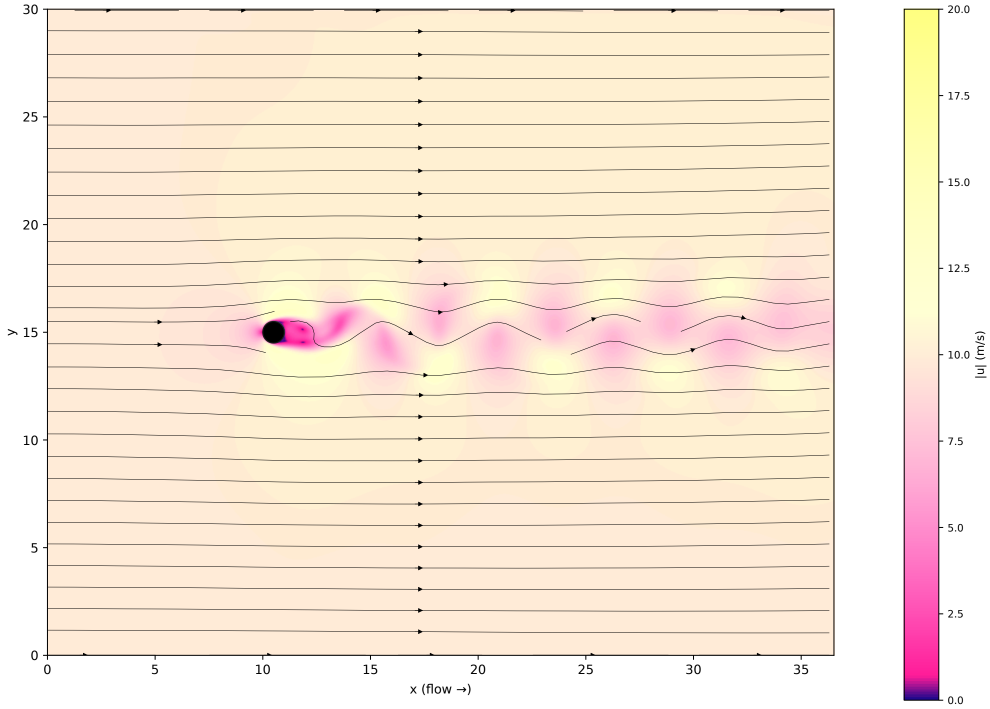

Figure 8: Full-domain speed field with streamlines.

5.0.3. Vorticity (full domain)

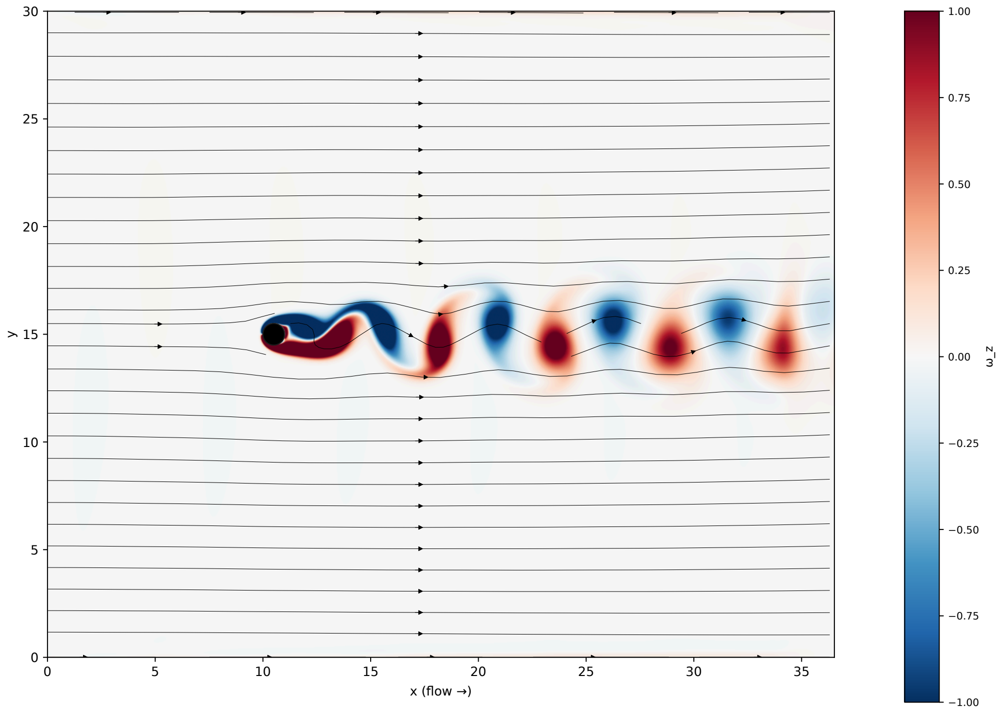

Figure 9: Full-domain normalized vorticity.

6. References

[1] Krüger, T., Kusumaatmaja, H., Kuzmin, A., Shardt, O., Silva, G., & Viggen, J. R. (2017). **The Lattice Boltzmann Method: Principles and Practice.** Springer. ISBN 978-3-319-44647-9.

[2] Henderson, R. (1995). Details of the drag curve near the onset of vortex shedding. **Physics of Fluids**, 7(9), 2102–2104.

[3] Sohankar, A., Norberg, C., & Davidson, L. (1998). Low-Reynolds-number flow around a square cylinder at incidence: study of blockage, onset of vortex shedding and outlet boundary condition. **International Journal for Numerical Methods in Fluids**, 26(1), 39–56.

[4] Franke, J., Hellsten, A., Schlünzen, H., & Carissimo, B. (2007). Best practice guideline for the CFD simulation of flows in the urban environment. COST Action 732.

[5] Roshko, A. (1961). Experiments on the flow past a circular cylinder at very high Reynolds number. **Journal of Fluid Mechanics**, 10(3), 345–356.